Food and Chemical Toxicology 131 (2019) 110527

Contents lists available at ScienceDirect

Food and Chemical Toxicology

journal homepage: www.elsevier.com/locate/foodchemtox

Activation of the p38/MAPK pathway regulates autophagy in response to the CYPOR-dependent oxidative stress induced by zearalenone in porcine intestinal epithelial cells

Tongtong Shen[a], Yufan Miao[a], Chenchen Ding[a], Wentao Fan[a], Shuhui Liu[a], Yanan Lv[a], Xiaona Gao[a], Marthe De Boevre[b], Liping Yan[a], Sheila Okoth[c], Sarah De Saeger[b], Suquan Song[a,*]

[a] MOE Joint International Research Laboratory of Animal Health and Food Safety, College of Veterinary Medicine, Nanjing Agricultural University, Nanjing, 210095, PR China

[b] Centre of Excellence in Mycotoxicology and Public Health, Department of Bioanalysis, Faculty of Pharmaceutical Sciences, Ghent University, Ottergemsesteenweg 460, B-9000 Ghent, Belgium

[c] School of Biological Sciences, University of Nairobi, Nairobi, Kenya

ARTICLE INFO

Keywords:
Zearalenone
Oxidative stress
Autophagy
CYPOR
p38/MAPK

ABSTRACT

Zearalenone (ZEA) can widely contaminate crops and agricultural products. The ingestion of ZEA-contaminated food or feed affects the integrity and functions of the intestines. In this study, we aimed to find the potential protective mechanism against ZEA ingestion. We found that ZEA induced cell death in IPEC-J2 cells. Meanwhile, the cytoprotective autophagy was activated in ZEA-treated cells. Further studies demonstrated that a p38/MAPK inhibitor down-regulated autophagy and increased cell death compared to those of the controls. Furthermore, ZEA could induce the accumulation of ROS, and eliminating ROS with NAC resulted in a decline in cell death, p38/MAPK phosphorylation, and the expression of LC3-II compared to those of ZEA-group. In addition, cytochrome P450 reductase (CYPOR) was significantly increased in ZEA-treated cells compared to that in the controls, and an inhibitor of CYPOR decreased ROS levels and mitigated cell death compared to those of the ZEA-group. More importantly, we found that blocking both p38/MAPK signalling and autophagy could enhance CYPOR expression and elevate ROS levels. Overall, our study indicated that the p38/MAPK pathway could activate protective autophagy in response to the CYPOR-dependent oxidative stress that was induced by ZEA in IPEC-J2 cells.

1. Introduction

Zearalenone (ZEA) is a nonsteroidal estrogenic mycotoxin that is mainly generated by several Fusarium species and can widely contaminate the crops and agricultural products (Kouadio et al., 2005). Growing evidence has shown that ZEA exposure could cause various toxic effects in human and animals, including reproductive toxicity, hepatotoxicity, teratogenesis, nephrotoxicity and carcinogenicity (Abrunhosa et al., 2016; Wentzel et al., 2017). Thus, ZEA has been listed as a group III carcinogen by the International Agency for Research on Cancer (De Ruyck et al., 2015). Due to the estrogen like structure and effect of ZEA, female reproductive system is always considered to be the major target organ of ZEA. However, because there are many estrogen receptor-positive cells, such as macrophages or epithelium, in the intestines (Kawano et al., 2004; Wada-Hiraike et al., 2006), ZEA may also affect the integrity and functions of the intestines. When ZEA-contaminated food or feed is ingested, the intestine will be directly exposed to high levels of ZEA. Some studies proved that ZEA could damage the intestinal villous structure in rats (Liu et al., 2014), affect the intestinal epithelial integrity in swine (Marin et al., 2015), and induce intestinal inflammation in mice (Fan et al., 2018). In our previous studies, we have proven that ZEA could decrease antioxidant enzyme activity and promote the production of reactive oxygen species (ROS), leading to oxidative stress in porcine intestinal epithelial cells, but the regulatory mechanism of ROS has not been well elucidated (Fan et al., 2017).

Cytochrome P450 (CYP450) enzymes serve as terminal oxidases in the mixed-function oxidase system for metabolizing various endogenous substrates and xenobiotics including drugs and toxins (Xing et al., 2013). CYP450 enzymes are the main sources of ROS production in the body. Upon encountering substrates, CYP450 will consume nicotinamide adenine dinucleotide phosphate (NADPH) resulting in

* Corresponding author.
E-mail address: suquan.song@njau.edu.cn (S. Song).

https://doi.org/10.1016/j.fct.2019.05.035
Received 6 April 2019; Received in revised form 19 May 2019; Accepted 23 May 2019
Available online 05 June 2019
0278-6915/

Abbreviations

ACTB	beta Actin
ATG	autophagy-related
Bax	Bcl-2-associated X protein
BECN1	Beclin 1
Bcl-2	B-cell lymphoma-2
caspase	cysteine-aspartic protease
CQ	chloroquine
CYP450	cytochrome P450
CYPOR	cytochrome P450 reductase
DAPI	4′,6-diamidino-2-phenylindole
LC3	microtubule-associated protein 1 light chain 3
MAPK	mitogen-activated protein kinase
MTT	3-(4,5-dimethylthiahiazol-2-y1)-2,5-diphenyltetrazolium bromide
NAC	N-acetyl-L-cysteine
Rap	rapamycin
ROS	reactive oxygen species
SB203580	4-[4-(4-fluorophenyl)-2-(4-methylsulfinylphenyl) -1H-imidazole-5-yl]pyridine
siRNA	small interfering RNA
SQSTM1	sequestosome-1
ZEA	Zearalenone
Z-VAD-FMK	N-Benzyloxycarbonyl-Val-Ala-Asp (O-Me) fluoromethyl ketone
3-MA	3-methyladenine
7-ER	7-ethoxyresorufin

continuous ROS generation (He et al., 2017). The ROS formation induced by CYP450 is influenced by the substrates and isoenzymes that are used. For example, it was reported that HepG2 cell lines could express CYP2E1 to induce high ROS generation resulting in cell toxicity after ethanol stimulation (Cederbaum et al., 2009). Benzo(a)pyrene induced CYP1A1 activation to generate ROS, promoting HIV-1 replication (Ranjit et al., 2018). In the porcine intestine, there are nine common CYP450s (Nielsen et al., 2017; Xie et al., 2016), including CYP1A1, CYP1B1, CYP2A19, CYP2E1, CYP3A29, CYP3A46, CYP11A1, CYP19A1, and CYPOR. However, which kinds of enzymes are involved in the metabolism of ZEA in IPEC-J2 cells is unknown.

ROS formation and oxidative stress have been proven to be involved in the regulation of programmed cell death by apoptosis and/or necrosis. In addition, ROS can activate autophagy in different types of somatic cells (Navarro-Yepes et al., 2014). Autophagy is an intracellular degradation system that delivers damaged organelles or cytoplasmic proteins to lysosomes through autophagosomes in cells to maintain cellular homeostasis and is considered to be protective, ameliorating toxicity and inhibiting cell death (Malaviya et al., 2014). Some studies proved that ZEA could induce cytoprotective autophagy in cardiac cells and rat Leydig cells to inhibit cell apoptosis (Ben Salem et al., 2017; Wang et al., 2014), while other studies confirmed that ZEA-induced autophagy could cause oxidative stress and destroy the cytoskeletal structure in mouse Sertoli cells (Zheng et al., 2018). The contradictory results from these studies suggested that the role of autophagy in ZEA treatment was related to the cells types. Therefore, it is of great significance to investigate the role of autophagy upon ZEA exposure in porcine intestinal cells.

As reported, the mitogen-activated protein kinases (MAPK) pathway could mediate toxins related autophagy (Wu et al., 2017). The MAPK pathways comprise a family of signalling proteins that convert extracellular stimuli into the activation of intracellular transduction pathways via phosphorylation of a cascade of substrates (Ayroldi et al., 2012). The three important subfamilies of MAPK signalling, the extracellular-signal-regulated kinase (ERK), c-jun N-terminal kinase (JNK), and p38 signalling pathways, have different roles in the process of autophagy. It was reported that ERK/MAPK could regulate autophagy to promote porcine intestinal epithelial cell survival upon ochratoxin A toxicity (Wang et al., 2018a). The JNK/MAPK signalling pathway plays a critical role in autophagy induction by fumonisin B1 exposure (Yin et al., 2016). It was also proved that p38/MAPK mediated the crotoxin-induced autophagy of human lung carcinoma SK-MES-1 cells in vitro (Han et al., 2014). However, which kinds of MAPK signalling are involved in autophagy regulation after ZEA exposure are unknown.

In the present study, we aimed to investigate the toxic effect and its molecular mechanism of ZEA on IPEC-J2 cells. Our research will ascertain the relationship among CYPOR, oxidative stress and autophagy in ZEA-induced intestinal toxicity. Additionally, it is of great significance for the study of the potential connections between exposure of mycotoxins and human chronic intestinal diseases.

2. Materials and methods

2.1. Antibodies and reagents

ZEA was purchased from Pribolab (Qing Dao, China). The p38/MAPK inhibitor SB203580 (A8254), autophagy inhibitor 3-methyladenine (A8353), caspase inhibitor Z-VAD-FMK (A1902), and phos-tag-Acrylamide (F4002) were obtained from APExBIO (Houston, TX, USA). The autophagy inhibitor chloroquine (MZ3401) was provided by Mao KangBio (Shanghai, China). The CYPOR inhibitor 7-Ethoxyresorufin (R131523) was obtained from Aladdin (Shanghai, China). The autophagy activator rapamycin (R8140) was purchased from Solarbio (Beijing, China). Anti-LC3B (ab192890) antibody was provided by Abcam (Cambridge, UK). The anti-ATG5 (D5F5U), anti-SQSTM1/p62 (D5E2), anti-β-Actin (ACTB) (13E5), HRP-labelled anti-rabbit IgG (7074) or anti-mouse IgG (7076) antibodies were obtained from Cell Signalling Technology (Beverly, MA, USA). Anti-p38 (sc-7972) and anti-CYPOR (sc-25270) antibodies were purchased from Santa Cruz Biotechnology (Dallas, TX, USA).

2.2. Cell culture and treatments

The porcine intestinal epithelium (IPEC-J2) cells were cultured in Dulbecco's modified Eagle's medium (DMEM) (Basal Media, Shanghai, China) containing 10% fetal bovine serum (BI, Shanghai, China) and 1% 100 × penicillin-streptomycin solution (Sangon, Shanghai, China). The cells were cultured at 37 °C in 5% CO_2. When the cell density reached 50–60% confluence, the culture medium was changed before treatment with ZEA and/or other agents. The ZEA concentrations used in our study are justified based on the presence of as high as 600 mg/kg of ZEA in grain commodities in India as measured by JECFA (JECFA, 2000). Such high levels can easily translate to very high concentrations of ZEA in the intestinal lumen to which the epithelial cells are exposed.

2.3. Cell viability and cell death measurement

Cell viability was measured with MTT assays (Solarbio, Beijing, China). The relative cell viability (%) is represented as the percentage of treated cells compared to the untreated control cells. Cell death was measured by flow cytometry (BD Accuri® C6 Flow cytometer, Franklin Lake, NJ, USA) or fluorescence microscopy (Nikon TI-S, Tokyo, Japan) using an Annexin V/ANXA5-FITC/PI staining kit (YEASEN, Shanghai, China).

2.4. Reverse transcription PCR and quantitative real-time PCR

Total RNA from cells was isolated and reverse transcribed into

cDNA. Real-time PCR was performed using the SYBR qPCR Master Mix (Vazyme, Nanjing, China). The mRNA expressions levels were evaluated with the comparative Ct method and normalized to the endogenous levels of ACTB. The primer sequences used for PCR are shown in Table S1.

2.5. Assessment of ROS generation

The ROS level was analysed using a DCFH-DA probe (Beyotime, Shanghai, China). DCFH-DA (10 μM) was added to cells and incubated at 37 °C for 30min in the dark. Then the fluorescence signals of DCF were detected by flow cytometry.

2.6. Western blot analysis

Cells were lysed in RIPA buffer and the protein concentrations were determined with bicinchoninic acid. Then, the lysates were separated by 12% SDS-PAGE and transferred onto 0.2 μm nitrocellulose membranes (GE, MA, USA). The membranes were blocked and incubated with primary antibodies at 4 °C overnight. After incubation with HRP-labelled secondary antibodies at 37 °C for 1 h, the protein bands were visualized using an enhanced chemiluminescence kit (Vazyme, Nanjing, China).

2.7. Transient transfection of plasmids DNA and small interfering RNA (siRNA)

Cationic liposomal transfection reagents Lipofectamine 2000 has

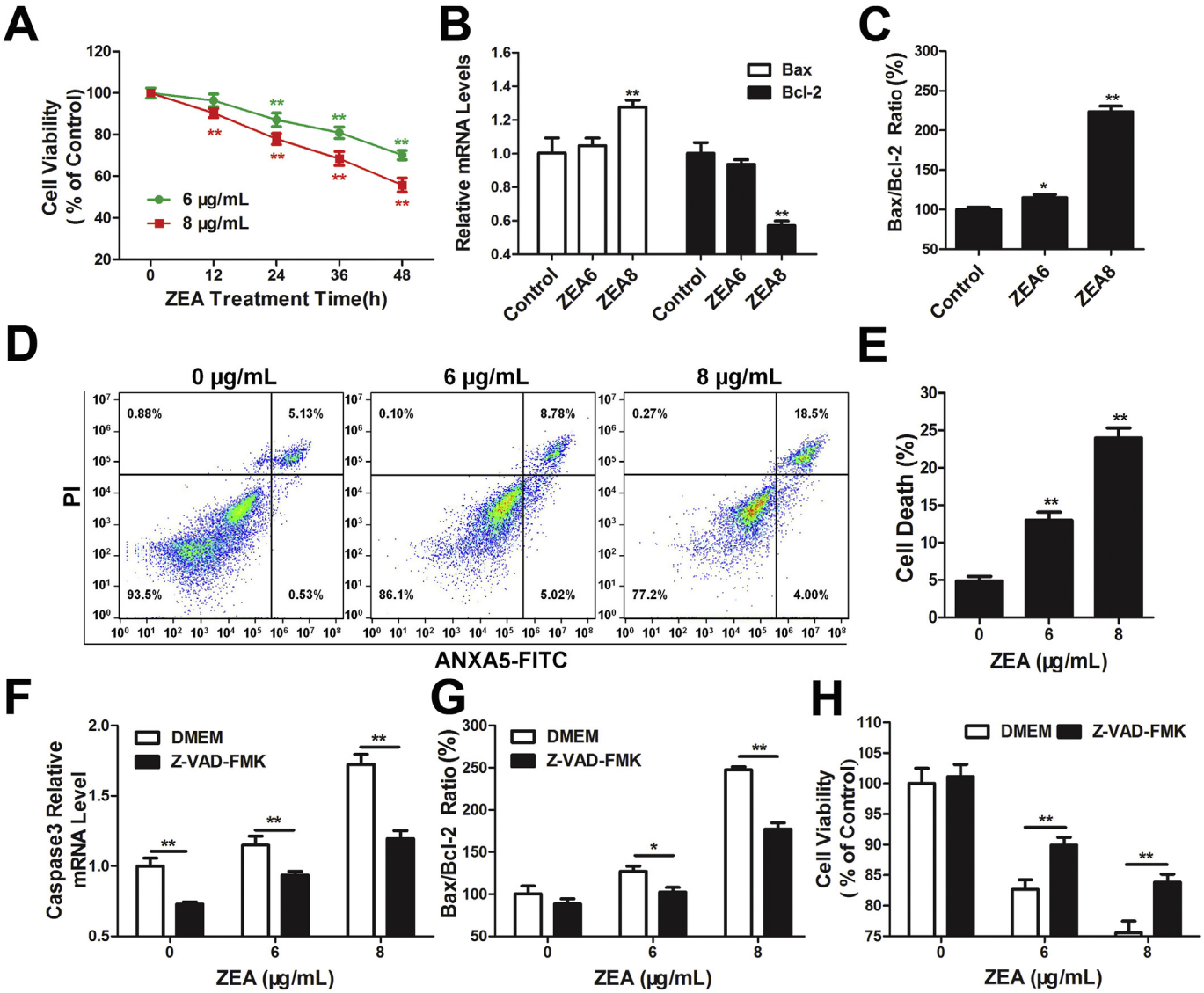

Fig. 1. ZEA induced caspase-dependent cell death in IPEC-J2 cells. (**A**) MTT assays were used to measure the cell viability of IPEC-J2 cells after 0 h, 12 h, 24 h, 36 h, and 48 h of ZEA (0, 6, and 8 μg/mL) treatment. (**B, C**) IPEC-J2 cells were treated with ZEA (0, 6, and 8 μg/mL) for 24 h. Bax and Bcl-2 mRNA expression were measured with real-time PCR. The ratio of Bax/Bcl-2 was the calculated as the ratio of its transcriptional levels. Control represents DMEM treatment. ZEA6 represents 6 μg/mL ZEA and ZEA8 represents 8 μg/mL ZEA. (**D, E**) IPEC-J2 cells were treated with different concentrations of ZEA (0, 6, and 8 μg/mL) for 24 h after being subjected to ANXA5-FITC/PI staining. The cells were analysed by flow cytometry. Unstained cells (negative for ANXA5-FITC and PI) were alive, while the others were dead. (**F-H**) The cells were pretreated with or without pan-caspase inhibitor Z-VAD-FMK (10 μM) for 3 h, and then treated with ZEA (0, 6, and 8 μg/mL) for 24 h. Then, (**F**) the relative mRNA level of caspase3, and (**G**) the ratio of Bax/Bcl-2 levels were analysed by real-time PCR and normalized to those of the control. (**H**) Effects of Z-VAD-FMK on the cell viability of IPEC-J2 cells treated with ZEA. The cell viability was measured with a MTT assay. Data are shown as the means ± standard deviations of three independent experiments, $^{*}P < 0.05$, $^{**}P < 0.01$.

been widely used to express exogenous genes within eukaryotic cells, due to their low toxicity, ease of use, and high degree of success. In this study, in order to improve the efficiency, Lipofectamine 2000 reagent were used to transfect the plasmid DNA and small interfering RNA (siRNA). For transfection of plasmids DNA, IPEC-J2 cells were transfected with Lipofectamine 2000 (Invitrogen, Carlsbad, Cal, USA) and EGFP-LC3B or pmCherry-EGFP-LC3B plasmids (Miao LingBio, Wuhan, China) according to the manufacturer's protocol. The cells were fixed with 4% paraformaldehyde at 37 °C for 30min and then counterstained with 4′, 6-diamidino-2-phenylindole (DAPI). The fluorescence signals were visualized with an Olympus Fluoview FV3000 Laser scanning confocal microscope (Olympus, Tokyo, Japan). For transient transfection of siRNA, the sense strand of siATG5 (5′-GCUUCGAGAUGUGUGG UUUtt-3′) and the control universal siRNA (Con Si) were purchased from General Biosystems (Chuzhou, China). A total of 50 nM of siATG5 and Con Si were transfected into IPEC-J2 cells with Lipofectamine 2000 reagent in Opti-MEM when the cell density reached nearly 30–50% confluence. The ATG5 knockdown was validated using western blotting.

2.8. Statistical analysis

The results are presented as the mean ± SD of at least three independent experiments. The prominent differences in the data were evaluated with SPSS 17.0 software (SPSS, USA), and analysed with the ANOVA. The differences were regarded as significant at *P < 0.05, and **P < 0.01.

3. Results

3.1. ZEA induced caspase-dependent cell death in IPEC-J2 cells

To investigate the cytotoxicity of ZEA exposure in IPEC-J2 cells, the MTT assay was used to evaluate the viability of IPEC-J2 cells at 0 h, 12 h, 24 h, 36 h, and 48 h after treatment with 6 μg/mL or 8 μg/mL ZEA. As shown in Fig. 1A, the cell viability gradually decreased in a time-dependent and dose-dependent manner in the treatment groups compared to that of the controls. To further investigate the overall cytotoxicity of ZEA in IPEC-J2 cells, we measured the transcription levels of

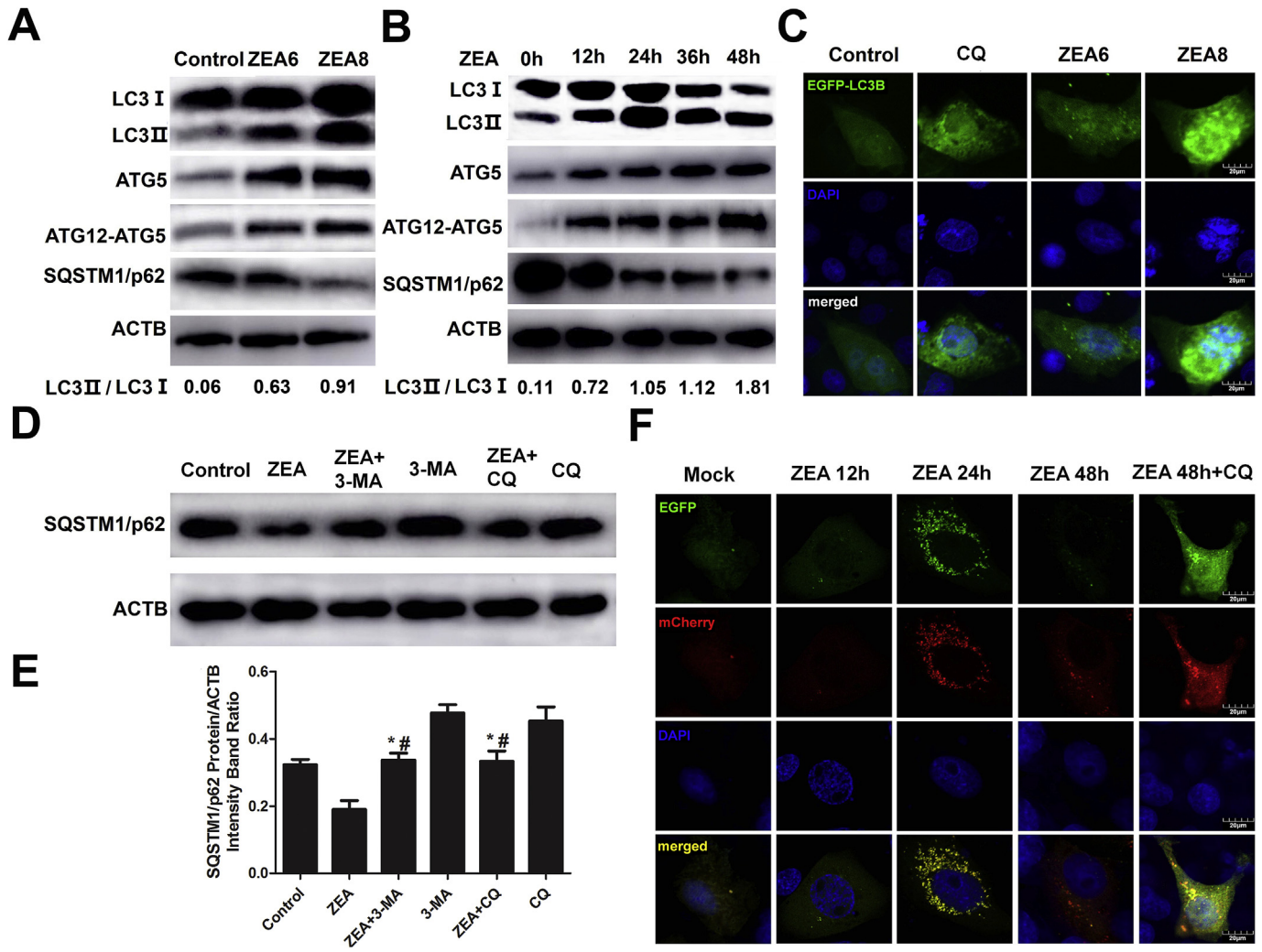

Fig. 2. ZEA induced autophagy and activated autophagic flux in IPEC-J2 cells. (**A, B**) IPEC-J2 cells were treated with ZEA (0, 6, and 8 μg/mL) for 24 h or treated with ZEA (8 μg/mL) for 0 h, 12 h, 24 h, 36 h, and 48 h. The expression of LC3, ATG5, ATG12–ATG5, SQSTM1/p62, and ACTB were analysed by Western blot. (**C**) IPEC-J2 cells were transfected with EGFP-LC3B for 24 h, followed by ZEA or CQ (50 nM) treatment for 24 h and were stained with DAPI. The fluorescence signals were visualized by confocal immunofluorescence microscopy. Bars: 20 μm. (**D, E**) Effect of 3-MA (5 mM) and CQ (50 nM) treatment on the expression of SQSTM1/p62 in the presence or absence of ZEA (8 μg/mL, 24 h). *$P < 0.05$ vs ZEA group, #$P < 0.05$ vs autophagy inhibitor alone treatment group. (**F**) IPEC-J2 cells were transfected with pmCherry-EGFP-LC3B for 6 h, followed by treatment with 8 μg/mL ZEA for 12 h, 24 h, and 48 h, or with 8 μg/mL ZEA and CQ for 48 h, and were then stained with DAPI. The fluorescence signals were visualized by confocal immunofluorescence microscopy. Bars: 20 μm. Control represents DMEM treatment. ZEA6 represents 6 μg/mL ZEA, and ZEA8 represents 8 μg/mL ZEA. Data are shown as the means ± standard deviations of three independent experiments, *$P < 0.05$, **$P < 0.01$.

Bax and Bcl-2. As shown in Fig. 1B, with the increase of the ZEA concentration, the mRNA level of Bax increased, whereas that of Bcl-2 decreased, compared to those of the controls. Therefore, the ratio of Bax to Bcl-2 increased accordingly (Fig. 1C). Simultaneously, the ANXA5-FITC/PI staining assays indicated the significant cell death in response to ZEA exposure compared to that of the controls (Fig. 1D and E). Furthermore, before treatment by ZEA, the cells were pretreated with a caspase inhibitor, Z-VAD-FMK, to determine the involvement of caspase activation in ZEA-induced cell death. The result showed that the caspase inhibitor could inhibit the mRNA expression of caspase3 and reduce the ratio of Bax to Bcl-2 compared to the controls (Fig. 1F and G), while promoting the cell viability (Fig. 1H) in ZEA-treated cells, suggesting caspase-dependent cell death was induced by ZEA in IPEC-J2 cells.

3.2. ZEA induced autophagy in IPEC-J2 cells

In this study, with the increase of the ZEA concentration, the mRNA level (Fig. S1A, B) and protein expressions (Fig. 2A) of LC3II and ATG5 were obviously upregulated, together with a decrease in LC3I expression, compared with those of the controls. Additionally, an indicator of the early stages of autophagy, BECN1, was upregulated (Fig. S1A, B), and the marker for the autophagy-mediated protein degradation pathway, SQSTM1/p62, was downregulated (Fig. 2A) in the treatment group compared to those of the controls. The level of the ATG12-ATG5 complex was increased in ZEA-treated cells (Fig. 2A) compared to that of the controls. Furthermore, ZEA induced accumulation of LC3II, ATG5, and the ATG12-ATG5 complex in a time-dependent manner in IPEC-J2 cells, along with a decrease in SQSTM1/p62 expression (Fig. 2B), compared to those of the controls. The formation of EGFP-LC3B puncta was examined in ZEA-treated cells, and the number of LC3B puncta was significantly increased compared with that in the control cells (Fig. 2C).

We then monitored the autophagic flux in ZEA (8 μg/mL, 24 h)-treated cells. The autophagy inhibitors 3-MA or CQ were used. As we know, 3-MA can inhibit autophagosome by suppressing class III phosphatidylinositide 3-kinases (PI-3K) and CQ can inhibit autophagosome fusion with lysosomes, thereby blocking degradation at the late stage. As shown in Fig. 2D and E, ZEA treatment alone decreased the expression of SQSTM1/p62 compared to that of the controls. When treated with the autophagy inhibitors of 3-MA or CQ, the SQSTM1/p62 expression in ZEA-treated cells were significantly increased, suggesting that ZEA effectively induced autophagy. To further confirm this observation, the mCherry-EGFP-LC3B plasmid was used to monitor autophagic flux. As shown in Fig. 2F, the green and red fluorescent puncta colocalized in the ZEA-treated IPEC-J2 cells at 24 h. At 48 h, red fluorescent puncta were still observed, and green fluorescent puncta were quenched. However, the addition of CQ recovered the green fluorescent puncta and increased the yellow puncta in ZEA-treated IPEC-J2 cells compared to those of the controls (Fig. 2F). These data

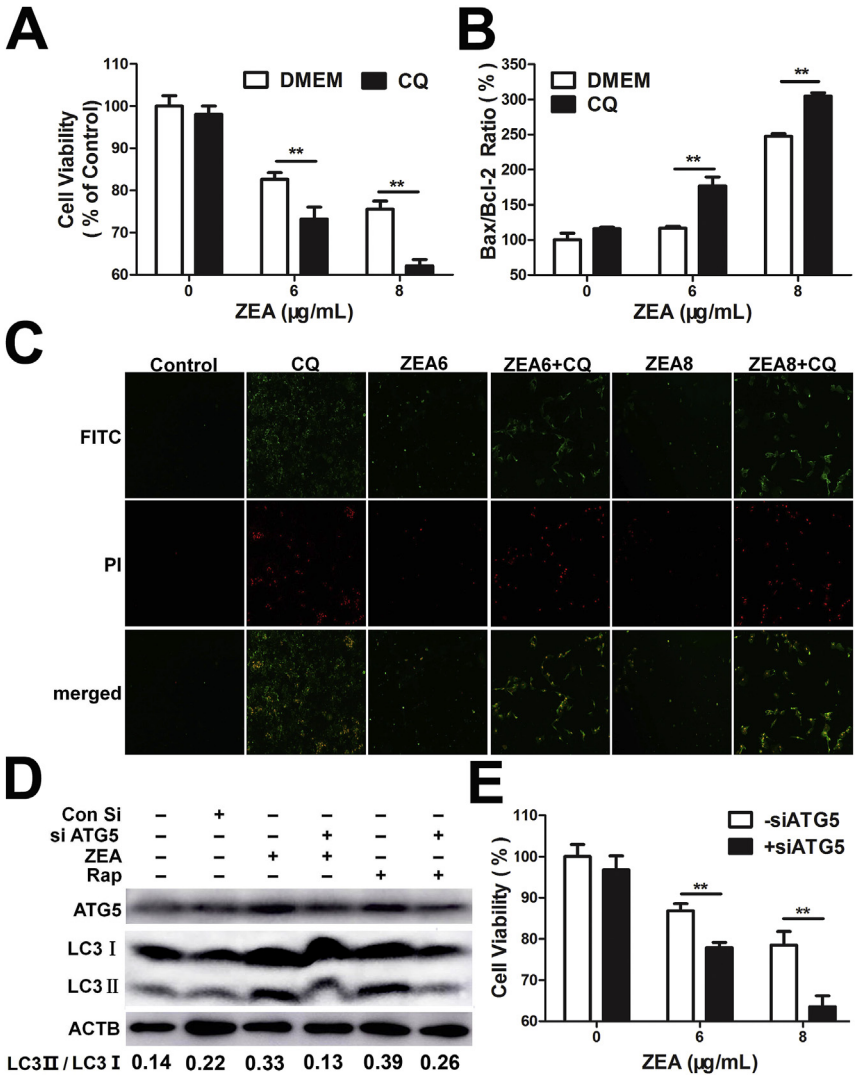

Fig. 3. Inhibition of autophagy promoted ZEA-induced cell death. IPEC-J2 cells were treated with chloroquine (CQ) (50 nM) in the presence or absence of ZEA (0, 6, and 8 μg/mL) for 24 h. Then, (**A**) the cell viability, and (**B**) Bax/Bcl-2 ratio was measured with the MTT and real-time PCR, and (**C**) cell death was measured using ANXA5-FITC/PI double staining and was analysed by fluorescence microscope. Cells that only exhibited green fluorescence were apoptotic. Double staining cells were necrotic (magnification, 20 ×). (**D**) ATG5 siRNA suppressed the expression of ATG5 and LC3 II. IPEC-J2 cells treated with rapamycin (10 nM) were used as a control. (**E**) Knockdown of ATG5 significantly increased the ZEA-induced decline of cell viability in IPEC-J2 cells. Data are shown as the means ± standard deviations of three independent experiments, $^{*}P < 0.05$, $^{**}P < 0.01$.

showed that ZEA treatment not only increased autophagosome formation but also completely induced autophagic flux.

3.3. Inhibition of autophagy promoted ZEA-induced cell death

We examined the effects of autophagy inhibitors CQ or siATG5 on ZEA-induced cell death to determine the role of autophagy in ZEA-induced cell death. As shown in Fig. 3A, the ZEA-treated cell viability was significantly reduced upon treatment with the autophagy inhibitors. Accordingly, the ratio of Bax/Bcl-2 and cell death increased in the treatment groups compared to those of the controls (Fig. 3B and C). Similarly, as expected, compared to those of the ZEA-group, ZEA failed to induce autophagy in siATG5 cells (Fig. 3D), and the ZEA-induced cell viability decreased, suggesting that the knockdown of ATG5 promoted cell death (Fig. 3E). Taken together, these results showed that autophagy played a protective role in ZEA-induced cell death.

3.4. The p38/MAPK pathway was involved in ZEA-induced autophagy

We examined the expression of the MAPK family proteins, the critical regulators of autophagy during mycotoxin exposure, including ERK, JNK, and p38, in ZEA-treated groups. Our results proved that in contrast to the other genes, the mRNA levels of p38 increased dramatically (Fig. 4A) with ZEA treatment. Additionally, the phosphorylation of p38/MAPK was increased in ZEA-treated cells (Fig. 4B). Then, we treated IPEC-J2 cells with ZEA and with the p38/MAPK inhibitor SB203580 and found that the ZEA-induced cell death was increased and cell viability was reduced (Fig. 4C and D) compared to those of the ZEA-group, which suggested that the p38/MAPK pathway played a critical role in ZEA-induced cell death. SB203580 was also used to investigate the role of p38/MAPK in ZEA-induced autophagy, and the result showed that the expressions of LC3II and SQSTM1/p62 were reversed in ZEA-treated cells (Fig. 4E). Meanwhile, SB203580 reduced the number of autophagy puncta in ZEA-treated cells (Fig. 4F). These results suggested that the p38/MAPK pathway participated in the regulation of ZEA-induced autophagy.

3.5. CYPOR-dependent oxidative stress regulated the p38/MAPK signalling pathway

In this study, DCFH-DA was used to detect the ROS level. As shown in Fig. 5A and B, the DCF fluorescence intensities were obviously increased in the ZEA groups compared to those of the controls. We investigated whether ROS contributed to ZEA-induced cell death. IPEC-J2 cells were treated with ZEA (8 μg/mL, 24 h) in the presence of N-acetylcysteine (NAC), a ROS inhibitor. As a result, compared with the ZEA group, NAC increased cell viability (Fig. 5C), inhibited cell death (Fig. S2A), and reduced the ratio of Bax/Bcl-2 (Fig. S2B). The results showed that ZEA induced oxidative stress-dependent cell death. In addition, compared to ZEA-group, the treatment of cells with ZEA and NAC

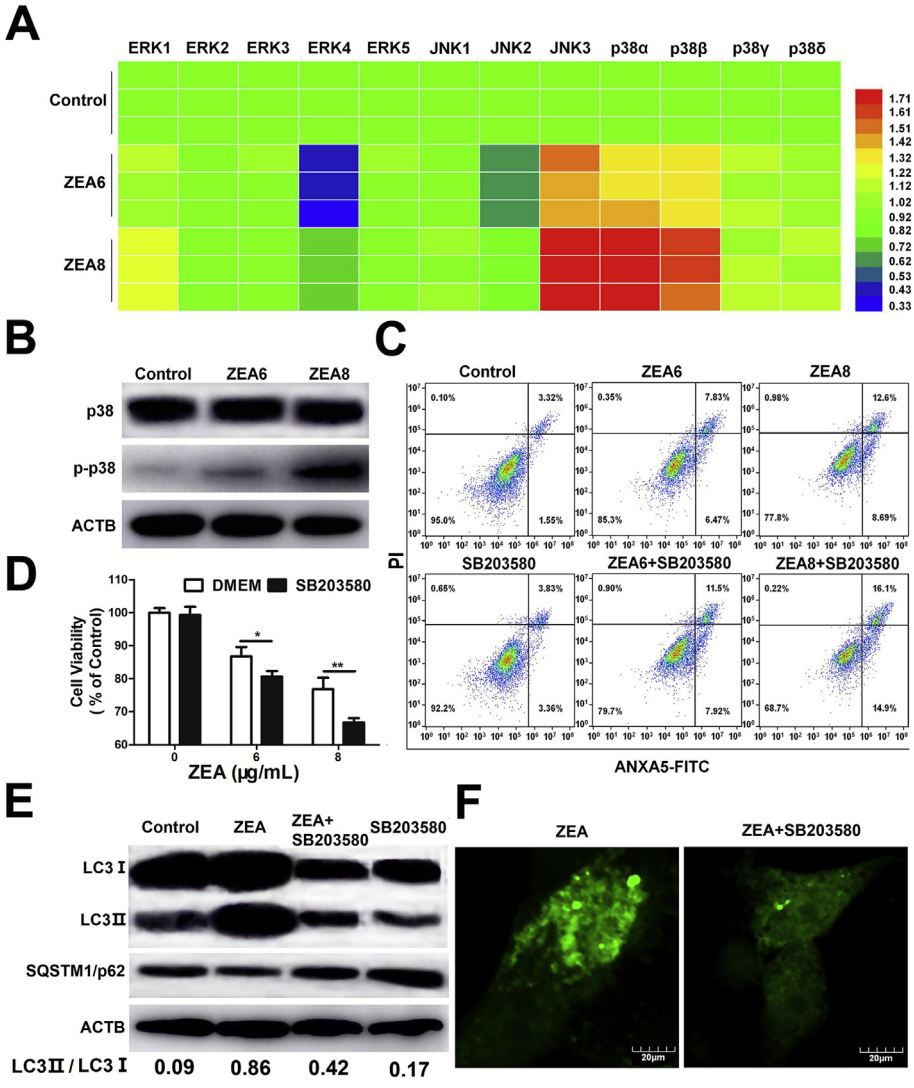

Fig. 4. The p38/MAPK inhibitor SB203580 reduced ZEA-induced autophagy. (**A**) The cells were treated with ZEA (0, 6, and 8 μg/mL) for 24 h and then the transcriptional levels of the ERK/MAPK, JNK/MAPK, and p38/MAPK genes were measured. (**B**) Phosphorylation of the p38/MAPK protein in ZEA-treated IPEC-J2 cells. (**C, D**) Effects of the combination of SB203580 (10 μM) and ZEA (0, 6, and 8 μg/mL) treatment for 24 h on cell death (**C**) and cell viability (**D**) in IPEC-J2 cells. (**E**) Western blot results for LC3 and SQSTM1/p62 in cells treated with both ZEA (8 μg/mL) and SB203580 (10 μM) or ZEA (8 μg/mL) alone for 24 h. (**F**) Decreased puncta distribution of EGFP-LC3B in cells treated with ZEA (8 μg/mL) and SB203580 (10 μM). Bar: 20 μm. Control represents DMEM treatment. ZEA6 represents 6 μg/mL ZEA, and ZEA8 represents 8 μg/mL ZEA. Data are shown as the means ± standard deviations of three independent experiments, $^{*}P < 0.05$, $^{**}P < 0.01$.

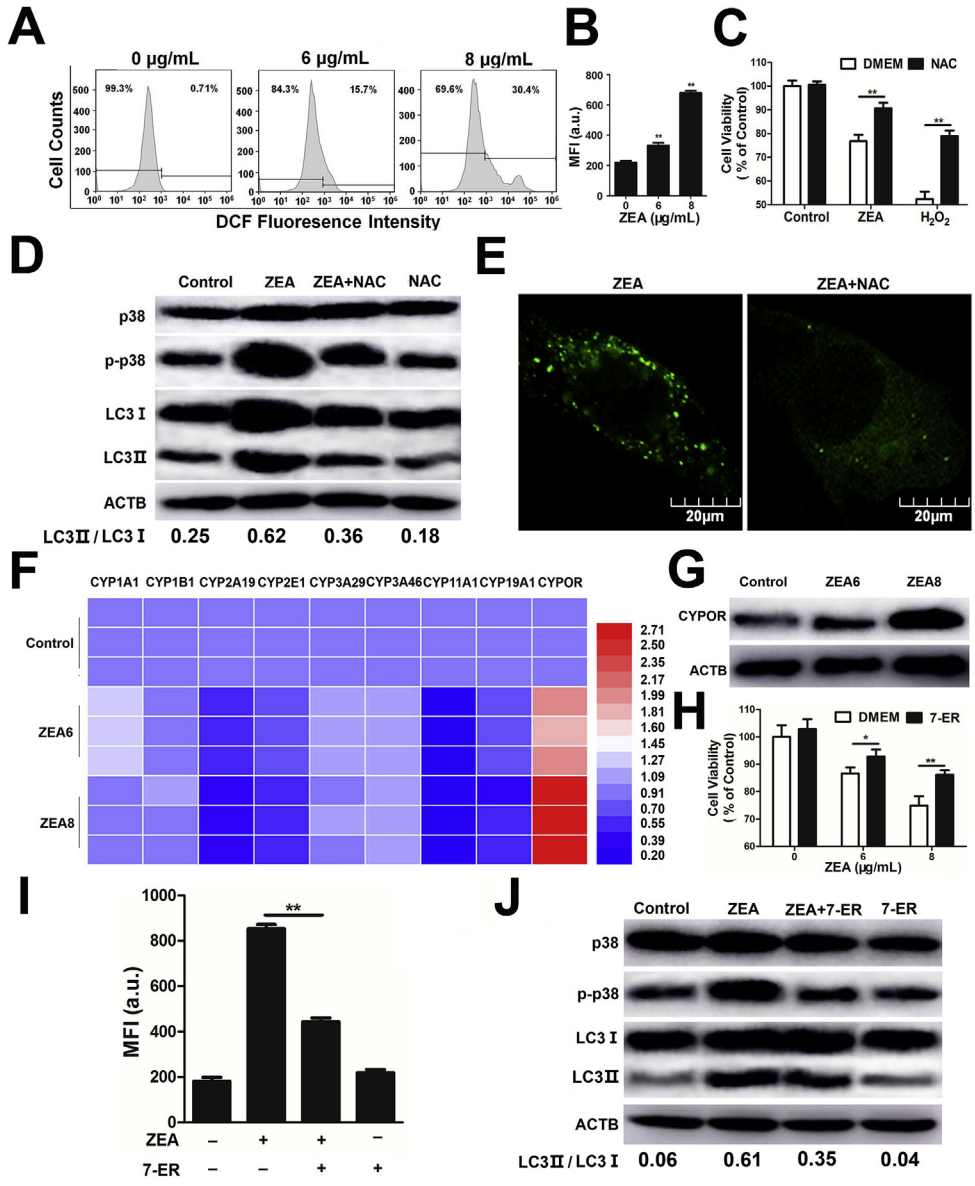

Fig. 5. CYPOR-dependent oxidative stress regulated the p38/MAPK signalling. ZEA induced cell death through oxidative stress. (**A**) Cells were treated with different concentrations of ZEA (0, 6, and 8 μg/mL) for 24 h. After an incubation with 10 μM DCFH-DA, the cells were washed and examined by flow cytometry. (**B**) The geometric mean of the fluorescence intensity (MFI) from DCF was analysed by FlowJo VX. (**C**) IPEC-J2 cells were treated with 8 μg/mL ZEA or with H_2O_2 in the absence or presence of NAC (5 mM) for 24 h, then the cell viability was measured with an MTT assay. (**D**) Western blot results of phosphorylation of p38/MAPK protein and LC3 in cells treated with both ZEA (8 μg/mL) and NAC (5 mM) or treated with ZEA (8 μg/mL) alone for 24 h. (**E**) NAC inhibited the formation of ZEA-induced autophagic puncta. Cells were treated with ZEA (8 μg/mL) and NAC (5 mM) for 24 h and were transfected with EGFP-LC3B plasmids. Bar: 20 μm. (**F, G**) The cells were treated with ZEA (0, 6, and 8 μg/mL) for 24 h. (**F**) The transcriptional levels of cytochrome P450 (CYP1A1, CYP1B1, CYP2A19, CYP2E1, CYP3A29, CYP3A46, CYP11A1, CYP19A1, and CYPOR) genes were measured by real-time PCR. (**G**) Western blot results for the CYPOR protein in ZEA-treated IPEC-J2 cells. (**H**) Cells were treated with the ZEA (0, 6, and 8 μg/mL) in the presence or absence of 7-ethoxyresorufin (7-ER, 10 μM) for 24 h, and cell viability was measured with an MTT assay. (**I, J**) Cells were treated with both ZEA (8 μg/mL) and 7-ER (10 μM) or were treated with ZEA (8 μg/mL) alone for 24 h. (**I**) The geometric mean of the fluorescence intensity from DCF was analysed by FlowJo VX. (**J**) Western blot results for the phosphorylation of the p38/MAPK protein and of the LC3 protein. Control represents DMEM treatment. ZEA6 represents 6 μg/mL ZEA, and ZEA8 represents 8 μg/mL ZEA. Data are shown as the means ± standard deviations of three independent experiments, $^{*}P < 0.05$, $^{**}P < 0.01$.

decreased p38/MAPK phosphorylation, LC3 II expression (Fig. 5D) and autophagic puncta formation (Fig. 5E), suggesting that ROS activated the p38/MAPK signalling pathway.

To investigate the effect of CYP450s on ZEA-induced oxidative stress, nine common CYP450s were measured at the transcriptional level in ZEA-treated IPEC-J2 cells. As shown in Fig. 5F, the mRNA levels of CYPOR were sharply increased in ZEA-treated cells compared to those of the controls. Next, the protein expression of CYPOR increased simultaneously compared to that of the controls (Fig. 5G). Furthermore, combined treatment with a CYPOR inhibitor (7-ethoxyresorufin, 7-ER) and ZEA was performed. The results demonstrated that cell viability was enhanced (Fig. 5H), cell death was decreased (Fig. S3A) and the Bax/Bcl-2 ratio was reduced (Fig. S3B) by 7-ER. In addition, 7-ER could reduce the DCF fluorescence intensities (Fig. 5I and Fig. S4) compared to those of the controls, suggesting that CYPOR could induce oxidative stress by stimulating ROS accumulation. Moreover, it was interesting to find that 7-ER could decrease the phosphorylation of p38/MAPK signalling (Fig. 5J), the expression of LC3 II (Fig. 5J) and the numbers of EGFP-LC3B puncta (Fig. S5). These results indicated that CYPOR could induce oxidative stress and thus mediate the p38/MAPK pathway.

3.6. The p38/MAPK pathway regulated autophagy against oxidative stress

We next investigated whether p38/MAPK signalling and autophagy were involved in the CYPOR-dependent oxidative stress induced by ZEA. First, IPEC-J2 cells were treated with both ZEA, together with SB203580 (Fig. 6A), siATG5 (Fig. 6B) or the autophagy inhibitor 3-MA (Fig. S6). The results indicated that, compared with the ZEA group, CYPOR expressions in all of treatment groups was increased, which proved that p38 and autophagy could inhibit CYPOR expression that was induced by ZEA. It is likely that the ROS levels were increased in these groups compared to that in the group treated with ZEA alone (Fig. 6C and D). Finally, cells were treated with in the presence of ZEA and SB203580. Compared with that of the group that received ZEA and SB203580 treatments, the cells that were also treated with 3-MA/siATG5 had ROS levels that were increased (Fig. 6C and D).

4. Discussion

In this study, we showed that ZEA inhibited cell viability and induced cell apoptosis and cell death in a dose- and time-dependent manner. These results were similar to the result of previous studies, in

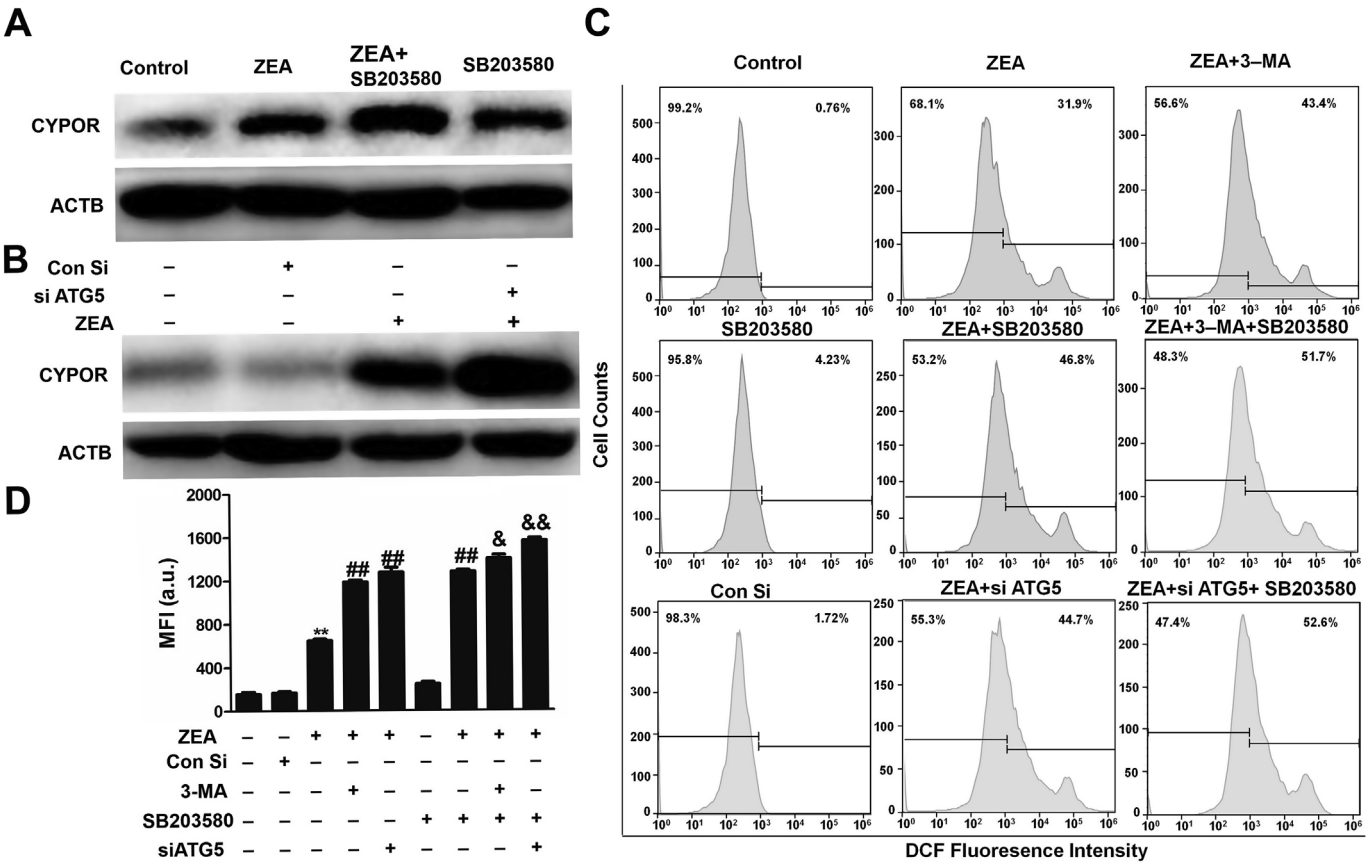

Fig. 6. p38/MAPK mitigated CYPOR-dependent oxidative stress through autophagy in ZEA-treated cells. (**A, B**) Western blot results for CYPOR in cells treated with both ZEA (8 μg/mL) and SB203580 (10 μM) (**A**) or siATG5 (50 nM) (**B**) for 24 h. (**C, D**) Cells were treated with ZEA (8 μg/mL) in the presence of 3-MA (5 mM), SB203580 (10 μM) or siATG5 (50 nM) for 24 h. (**C**) The DCF fluorescence intensity in IPEC-J2 cells was examined by flow cytometry. (**D**) Geometric mean of the fluorescence intensity from DCF was analysed by FlowJo VX. Data are the means ± standard deviations of three independent experiments, $^{**}P < 0.01$ vs control group, $\#\#P < 0.01$ vs ZEA group, & $P < 0.05$, && $P < 0.01$ vs ZEA + SB203580 group.

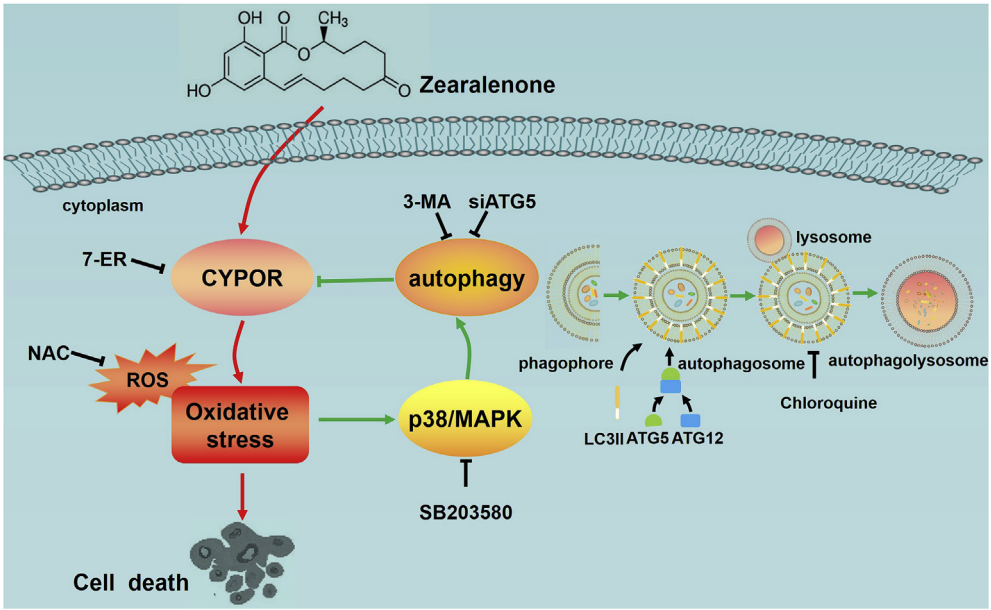

Fig. 7. Proposed toxicological mechanism of ZEA-induced cell death and a potential protective mechanism. ZEA induced CYPOR-derived oxidative stress, which in turn triggered the p38/MAPK pathway to regulate protective autophagy. Autophagy inhibited CYPOR to mitigate ZEA-induced oxidative stress.

which ZEA inhibited the proliferation and induced apoptosis in porcine small intestinal cells and in human neuroblastoma cells, mainly via excessive ROS production (Venkataramana et al., 2014; Wang et al., 2018b). Therefore, we used NAC to scavenge ROS and found that NAC increased cell viability and reduced cell death in ZEA-treated cells compared to those of the controls, which suggested that the ZEA-

induced IPEC-J2 cell death was mediated by ROS accumulation. As previously documented, in the CYP450-mediated metabolism of toxic substances, such as ochratoxin A, the catalytic activities of CYP450 required oxygen activation, which resulted in the production of ROS, generated toxic metabolisms, and increased the toxicity of toxins (Leung and Nieto, 2013; Tao et al., 2018). In this study, we first detected whether CYP450 enzymes played important roles in ZEA-induced intestinal toxicity. The result demonstrated that several intestinal CYP450s were changed in ZEA-treated cells at the transcriptional levels, including a sharp increase in CYPOR at both the mRNA and protein levels compared to those of the controls. Evidence has demonstrated that CYPOR received the electrons from reduced NADPH and supplied electrons to microsomal CYP450 to metabolize xenobiotics and steroid hormones (Xia et al., 2011), or offered electrons to many other proteins and small molecules substances (Pandey and Fluck, 2013). Therefore, the upregulation of CYPOR in ZEA-treated cells might be due to the induction by ZEA. However, this result is different from those of other studies, in which, CYP1A and CYP3A were shown to be involved in the oxidative damage of aflatoxin B1 and fumonisin B1 in rat spleen mononuclear cells (Mary et al., 2012) suggesting that the CYP450 activation varies according to the toxins.

Some studies have confirmed that autophagy could protect cells from the toxicity of mycotoxins, such as deoxynivalenol or T-2 toxin (Tang et al., 2015; Wu et al., 2019). In this study, we found that ZEA could induce autophagy and could completely induce autophagic flux in IPEC-J2 cells. In addition, the inhibition of autophagy or the knockdown of an autophagy gene with siATG5 could obviously reduce intestinal cell viability and aggravate cell death compared to those of the controls. That is, autophagy could protect IPEC-J2 cells against ZEA-induced cell death. This result was similar to that of a previous study, in which protective autophagy inhibited ZEA-induced apoptosis in mouse ovarian granulosa cells (Chen et al., 2019). As the MAPK pathway can mediate autophagy in ochratoxin A-treated cells (Wang et al., 2018a), we examined the role of this signalling pathway in ZEA-treated cells. We found that the p38/MAPK transcriptional levels and p-p38 were enhanced with the induction of ZEA compared to those of the controls. Furthermore, we confirmed that oxidative stress could activate the p38/MAPK signalling pathway and initiate autophagy in ZEA-treated cells. The results were different from those of another mycotoxin, deoxynivalenol, which activated only the JNK/MAPK pathway in mammalian cells (Li et al., 2018). In addition, it has been reported that in pig spleen, ZEA could suppress p38/MAPK, but could activate the JNK pathway (Pistol et al., 2015). Thus, we assume that different mycotoxins might have different activation mechanisms via the MAPK pathway and that the activation of the MAPK pathway was diverse in different organs after ZEA exposure.

It has been proven that the nuclear xenobiotic receptor pathway could modulate CYPOR after di (2-ethylhexyl) phthalate exposure in quails (Zhang et al., 2018). However, the understanding of the mechanism of CYPOR regulation is currently limited. In our study, we found that p38 inhibition and autophagy inhibition could enhance CYPOR expression, leading to ROS generation, thus, p38/MAPK signalling and autophagy played a key role in inhibiting CYPOR-dependent oxidative stress after ZEA treatment in porcine intestinal cells. Thus, our findings provide a new mechanism for CYPOR regulation during mycotoxin exposure in mammalian cells.

In summary, ZEA induces IPEC-J2 cell death through CYPOR-derived oxidative stress. Additionally, the ROS that is produced can trigger the p38/MAPK signalling pathway, which then activated p38/MAPK to regulate autophagy and protect intestinal cells from ZEA-induced oxidative stress. A possible toxicological mechanism of ZEA-induced cell death and a potential protective mechanism are shown in Fig. 7. Our findings provide a new insight into the mechanism underlying ZEA-induced porcine intestinal toxicity. Furthermore, autophagy is a possible target for therapeutic intervention against ZEA-induced intestinal injury.

Conflicts of interest

The authors announce that there are no conflicts of interest.

Acknowledgments

This study was supported by the National Key R&D Program (2016YFD0501009 and 2016YFD0501200), the Natural Science Foundation of Jiangsu Province (BK20161452), the Fundamental Research Funds for the Central Universities (KYZ201848), the NAU International Cooperation and Cultivation Project (2018-AF-20), the graduate student scientific research innovation projects of Jiangsu Province (KYCX18_0710), the Key Program of Science and Technology Planning of Guangdong Province (2017B020202010), and the Priority Academic Program Development of Jiangsu Higher Education Institutions.

Transparency document

Transparency document related to this article can be found online at https://doi.org/10.1016/j.fct.2019.05.035

Appendix A. Supplementary data

Supplementary data to this article can be found online at https://doi.org/10.1016/j.fct.2019.05.035.

References

Abrunhosa, L., Morales, H., Soares, C., Calado, T., Vila-Cha, A.S., Pereira, M., Venancio, A., 2016. A review of mycotoxins in food and feed products in Portugal and estimation of probable daily intakes. Crit. Rev. Food Sci. Nutr. 56, 249–265.

Ayroldi, E., Cannarile, L., Migliorati, G., Nocentini, G., Delfino, D.V., Riccardi, C., 2012. Mechanisms of the anti-inflammatory effects of glucocorticoids: genomic and non-genomic interference with MAPK signaling pathways. FASEB J. 26, 4805–4820.

Ben Salem, I., Boussabbeh, M., Pires Da Silva, J., Guilbert, A., Bacha, H., Abid-Essefi, S., Lemaire, C., 2017. SIRT1 protects cardiac cells against apoptosis induced by zearalenone or its metabolites alpha- and beta-zearalenol through an autophagy-dependent pathway. Toxicol. Appl. Pharmacol. 314, 82–90.

Cederbaum, A.I., Lu, Y., Wu, D., 2009. Role of oxidative stress in alcohol-induced liver injury. Arch. Toxicol. 83, 519–548.

Chen, F., Wen, X., Lin, P., Chen, H., Wang, A., Jin, Y., 2019. HERP depletion inhibits zearalenone-induced apoptosis through autophagy activation in mouse ovarian granulosa cells. Toxicol. Lett. 301, 1–10.

De Ruyck, K., De Boevre, M., Huybrechts, I., De Saeger, S., 2015. Dietary mycotoxins, co-exposure, and carcinogenesis in humans: short review. Mutat. Res. Rev. Mutat. Res. 766, 32–41.

Fan, W., Shen, T., Ding, Q., Lv, Y., Li, L., Huang, K., Yan, L., Song, S., 2017. Zearalenone induces ROS-mediated mitochondrial damage in porcine IPEC-J2 cells. J. Biochem. Mol. Toxicol. 31, e21944.

Fan, W.T., Lv, Y.A., Ren, S., Shao, M.Y., Shen, T.T., Huang, K.H., Zhou, J.Y., Yan, L.P., Song, S.Q., 2018. Zearalenone (ZEA)-induced intestinal inflammation is mediated by the NLRP3 inflammasome. Chemosphere 190, 272–279.

Han, R., Liang, H., Qin, Z.H., Liu, C.Y., 2014. Crotoxin induces apoptosis and autophagy in human lung carcinoma cells in vitro via activation of the p38MAPK signaling pathway. Acta Pharmacol. Sin. 35, 1323–1332.

He, L., He, T., Farrar, S., Ji, L., Liu, T., Ma, X., 2017. Antioxidants maintain cellular redox homeostasis by elimination of reactive oxygen species. Cell. Physiol. Biochem. 44, 532–553.

JECFA, 2000. Zearalenone. In: Joint FAO/WHO Expert Committee on Food Additives. Safety evaluation of certain food additives and contaminants. WHO/FAO Food additives Series 44. IPCS – International Programme on Chemical Safety. WHO, Geneva.

Kawano, N., Koji, T., Hishikawa, Y., Murase, K., Murata, I., Kohno, S., 2004. Identification and localization of estrogen receptor alpha- and beta-positive cells in adult male and female mouse intestine at various estrogen levels. Histochem. Cell Biol. 121, 399–405.

Kouadio, J.H., Mobio, T.A., Baudrimont, I., Moukha, S., Dano, S.D., Creppy, E.E., 2005. Comparative study of cytotoxicity and oxidative stress induced by deoxynivalenol, zearalenone or fumonisin B1 in human intestinal cell line Caco-2. Toxicology 213, 56–65.

Leung, T.M., Nieto, N., 2013. CYP2E1 and oxidant stress in alcoholic and non-alcoholic fatty liver disease. J. Hepatol. 58, 395–398.

Li, X.M., Mu, P.Q., Qiao, H., Wen, J.K., Deng, Y.Q., 2018. JNK-AKT-NF-kappa B controls P-glycoprotein expression to attenuate the cytotoxicity of deoxynivalenol in mammalian cells. Biochem. Pharmacol. 156, 120–134.

Liu, M., Gao, R., Meng, Q.W., Zhang, Y.Y., Bi, C.P., Shan, A.S., 2014. Toxic effects of maternal zearalenone exposure on intestinal oxidative stress, barrier function,

immunological and morphological changes in rats. PLoS One 9, e106412.
Malaviya, R., Laskin, J.D., Laskin, D.L., 2014. Oxidative stress-induced autophagy: role in pulmonary toxicity. Toxicol. Appl. Pharmacol. 275, 145–151.
Marin, D.E., Motiu, M., Taranu, I., 2015. Food contaminant zearalenone and its metabolites affect cytokine synthesis and intestinal epithelial integrity of porcine cells. Toxins 7, 1979–1988.
Mary, V.S., Theumer, M.G., Arias, S.L., Rubinstein, H.R., 2012. Reactive oxygen species sources and biomolecular oxidative damage induced by aflatoxin B1 and fumonisin B1 in rat spleen mononuclear cells. Toxicology 302, 299–307.
Navarro-Yepes, J., Burns, M., Anandhan, A., Khalimonchuk, O., del Razo, L.M., Quintanilla-Vega, B., Pappa, A., Panayiotidis, M.I., Franco, R., 2014. Oxidative stress, redox signaling, and autophagy: cell death versus survival. Antioxidants Redox Signal. 21, 66–85.
Nielsen, S.D., Bauhaus, Y., Zamaratskaia, G., Junqueira, M.A., Blaabjerg, K., Petrat-Melin, B., Young, J.F., Rasmussen, M.K., 2017. Constitutive expression and activity of cytochrome P450 in conventional pigs. Res. Vet. Sci. 111, 75–80.
Pandey, A.V., Fluck, C.E., 2013. NADPH P450 oxidoreductase: structure, function, and pathology of diseases. Pharmacol. Therapeut. 138, 229–254.
Pistol, G.C., Braicu, C., Motiu, M., Gras, M.A., Marin, D.E., Stancu, M., Calin, L., Israel-Roming, F., Berindan-Neagoe, I., Taranu, I., 2015. Zearalenone mycotoxin affects immune mediators, MAPK signalling molecules, nuclear receptors and genome-wide gene expression in pig spleen. PLoS One 10, e0127503.
Ranjit, S., Sinha, N., Kodidela, S., Kumar, S., 2018. Benzo(a)pyrene in cigarette smoke enhances HIV-1 replication through NF-kappaB activation via CYP-mediated oxidative stress pathway. Sci. Rep. 8, 10394.
Tang, Y.L., Li, J.J., Li, F.N., Hu, C.A.A., Liao, P., Tan, K.R., Tan, B., Xiong, X., Liu, G., Li, T.J., Yin, Y.L., 2015. Autophagy protects intestinal epithelial Cells against Deoxynivalenol toxicity by alleviating oxidative stress via IKK signaling pathway. Free Radic. Biol. Med. 89, 944–951.
Tao, Y., Xie, S., Xu, F., Liu, A., Wang, Y., Chen, D., Pan, Y., Huang, L., Peng, D., Wang, X., Yuan, Z., 2018. Ochratoxin A: toxicity, oxidative stress and metabolism. Food Chem. Toxicol. 112, 320–331.
Venkataramana, M., Chandra Nayaka, S., Anand, T., Rajesh, R., Aiyaz, M., Divakara, S.T., Murali, H.S., Prakash, H.S., Lakshmana Rao, P.V., 2014. Zearalenone induced toxicity in SHSY-5Y cells: the role of oxidative stress evidenced by N-acetyl cysteine. Food Chem. Toxicol. 65, 335–342.
Wada-Hiraike, O., Imamov, O., Hiraike, H., Hultenby, K., Schwend, T., Omoto, Y., Warner, M., Gustafsson, J.-Å., 2006. Role of estrogen receptor β in colonic epithelium. In: Proceedings of the National Academy of Sciences of the United States of America. vol. 103. pp. 2959–2964.
Wang, H., Li, H., Chen, X., Huang, K., 2018a. ERK1/2-mediated autophagy is essential for cell survival under Ochratoxin A exposure in IPEC-J2 cells. Toxicol. Appl. Pharmacol. 360, 38–44.
Wang, J., Li, M., Zhang, W., Gu, A., Dong, J., Li, J., Shan, A., 2018b. Protective effect of N-acetylcysteine against oxidative stress induced by zearalenone via mitochondrial apoptosis pathway in SIEC02 cells. Toxins 10, 407.
Wang, Y., Zheng, W., Bian, X., Yuan, Y., Gu, J., Liu, X., Liu, Z., Bian, J., 2014. Zearalenone induces apoptosis and cytoprotective autophagy in primary Leydig cells. Toxicol. Lett. 226, 182–191.
Wentzel, J.F., Lombard, M.J., Du Plessis, L.H., Zandberg, L., 2017. Evaluation of the cytotoxic properties, gene expression profiles and secondary signalling responses of cultured cells exposed to fumonisin B1, deoxynivalenol and zearalenone mycotoxins. Arch. Toxicol. 91, 2265–2282.
Wu, J., Zhou, Y., Yuan, Z., Yi, J., Chen, J., Wang, N., Tian, Y., 2019. Autophagy and apoptosis interact to modulate T-2 toxin-induced toxicity in liver cells. Toxins 11, 45.
Wu, Q., Wang, X., Nepovimova, E., Miron, A., Liu, Q., Wang, Y., Su, D., Yang, H., Li, L., Kuca, K., 2017. Trichothecenes: immunomodulatory effects, mechanisms, and anticancer potential. Arch. Toxicol. 91, 3737–3785.
Xia, C., Panda, S.P., Marohnic, C.C., Martasek, P., Masters, B.S., Kim, J.J., 2011. Structural basis for human NADPH-cytochrome P450 oxidoreductase deficiency. Proc. Natl. Acad. Sci. U. S. A. 108, 13486–13491.
Xie, F., Ding, X., Zhang, Q.Y., 2016. An update on the role of intestinal cytochrome P450 enzymes in drug disposition. Acta Pharm. Sin. B 6, 374–383.
Xing, H., Wang, H., Sun, G., Wu, H., Zhang, J., Xing, M., Xu, S., 2013. Antioxidant response, CYP450 system, and histopathological changes in the liver of nitrobenzene-treated drakes. Res. Vet. Sci. 95, 1088–1093.
Yin, S., Guo, X., Li, J., Fan, L., Hu, H., 2016. Fumonisin B1 induces autophagic cell death via activation of ERN1-MAPK8/9/10 pathway in monkey kidney MARC-145 cells. Arch. Toxicol. 90, 985–996.
Zhang, Y.Z., Zuo, Y.Z., Du, Z.H., Xia, J., Zhang, C., Wang, H., Li, X.N., Li, J.L., 2018. Di (2-ethylhexyl) phthalate (DEHP)-induced hepatotoxicity in quails (Coturnix japonica) via triggering nuclear xenobiotic receptors and modulating cytochrome P450 systems. Food Chem. Toxicol. 120, 287–293.
Zheng, W.L., Wang, B.J., Si, M.X., Zou, H., Song, R.L., Gu, J.H., Yuan, Y., Liu, X.H., Zhu, G.Q., Bai, J.F., Bian, J.C., Liu, Z.P., 2018. Zearalenone altered the cytoskeletal structure via ER stress- autophagy- oxidative stress pathway in mouse TM4 Sertoli cells. Sci. Rep. 8, 3320.